





Optics Letters

Spontaneous diametric-drive acceleration initiated by a single beam in a photonic lattice

YUMIAO PEI,¹  ZHAOYUAN WANG,¹ YI HU,^{1,*} CIBO LOU,² ZHIGANG CHEN,^{1,3,4}  AND JINGJUN XU^{1,5}

¹The MOE Key Laboratory of Weak-Light Nonlinear Photonics, TEDA Applied Physics Institute and School of Physics, Nankai University, Tianjin 300457, China

²Faculty of Science, Ningbo University, Ningbo 315211, China

³Department of Physics and Astronomy, San Francisco State University, San Francisco, California 94132, USA

⁴e-mail: zgchen@nankai.edu.cn

⁵e-mail: jjxu@nankai.edu.cn

*Corresponding author: yihu@nankai.edu.cn

Received 9 April 2020; revised 5 May 2020; accepted 5 May 2020; posted 5 May 2020 (Doc. ID 394838); published 1 June 2020

We demonstrate that a single Gaussian-like beam can self-bend during nonlinear propagation in a uniform photonic lattice. The two components of the beam experiencing normal and anomalous diffractions spontaneously separate and form a pair in a diametric-drive acceleration due to nonlinear action. Such a diametric drive generally describes a jointly accelerating behavior of two beams analogous to positive- and negative-mass objects. The influences of the initial momentum of the input beam and the nonlinear strength are considered in this process. We further realize a self-bending propagation for a partially coherent light beam and discuss the impact of incoherence on the acceleration strength. © 2020 Optical Society of America

<https://doi.org/10.1364/OL.394838>

Photonic lattices, periodically arranged and evanescently coupled waveguides, offer a versatile platform for shaping light propagations [1]. They bring about fruitful diffraction relationships giving birth to new control degrees of freedom that otherwise cannot be achieved in homogeneous media. To steer or switch a light beam in such optical structures, additional modulations have been widely employed since, in general, the momentum of an optical beam cannot be altered in a uniform lattice. A transverse “force” experienced by a light beam can be produced by properly chirping the waveguide width or the lattice spacing [2,3], by engineering the longitudinal modulation [4], or even by simply introducing some defects [5], to name just a few examples. These fixed structures face difficulties or limitations in achieving a tunable steering. To tune the transverse force, a temperature gradient across the lattice is employed via the thermal-optical effect [6,7], but this approach involves increased complexity of the device.

Alternatively, nonlinearity embedded in photonic lattices offers a flexible way for beam steering. An optical beam can be attracted or repelled by another one [8,9]. One can merely employ the phase or the spacing between them to switch the sign of the interaction force. Straightforwardly, optical power, which

can tune the nonlinear strength, is also routinely employed for the control of beam steering [10–12]. Quite recently, we demonstrated that two light beams can experience a jointly self-bending propagation in a uniform lattice [13], leading to a steering functionality that can only be realized in a non-uniform structure. Such a phenomenon, namely, diametric-drive acceleration, initially proposed in the temporal domain [14,15], is analogous to the interaction between positive- and negative-mass objects that break the action-reaction symmetry. It differs not only from the dynamics of linear self-accelerating beams whose “center of mass” evolves along a straight line [16], but also from their interactions [17] where action-reaction symmetry persists. Diametric-drive acceleration was also investigated recently in other physical systems [18,19] or in a coherent configuration [20] triggered by the counterintuitive dynamics brought by negative mass [21]. To realize a jointly accelerating propagation in a photonic lattice, the pattern of the two input beams should be properly designed aiming to match the lattice modes in the normal and anomalous diffraction regions. One may wonder if this mechanism enables an optical steering in a simpler manner, for instance, with a single-beam excitation.

In this Letter, we demonstrate that a single Gaussian-like beam can self-bend under the action of a nonlinearity in a uniform lattice. The constituting components of the beam experiencing diffractions of opposite signs undergo a separation and then form a pair of diametric-drive acceleration during nonlinear propagation. The acceleration strength can be tuned by the initial momentum of the input beam and the nonlinearity. Furthermore, we find that the spontaneous bending is possible in the framework of partially coherent propagation, where the acceleration strength is still appreciable, even for a modest degree of incoherence.

In a photonic lattice, normal and anomalous diffractions co-exist in the same transmission band (i.e., Bloch band), where they are separated by the zero-diffraction point. A typical diffraction relationship (propagation constant β versus transverse wave vector k_x) for a one-dimensional (1D) lattice is schematically shown in Fig. 1(a). A single beam, launched near

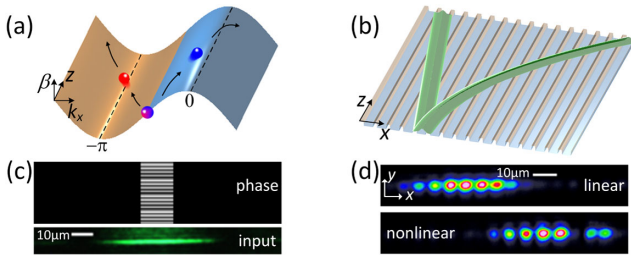


Fig. 1. (a) Schematic spectrum evolution (along the z direction) of a probe beam launched at a zero-diffraction point of a Bloch band (where the normal and anomalous diffraction regions are distinguished by blue and orange colors) during a spontaneous diametric-drive acceleration. The spectral components (denoted by red and blue spheres) experiencing different types of diffraction are expected to move along opposite directions. (b) Rectilinear propagation (left) in the absence of a nonlinearity and the diametric-drive acceleration (right) in a photonic lattice. (c) Phase pattern (upper panel, obtained by wrapping a vertically gradient phase between 0 and 2π) loaded onto an SLM for generating a Gaussian-like beam (bottom panel). (d) Captured linear and nonlinear output beam patterns.

the zero-diffraction point, can excite both diffraction regions [Fig. 1(a)], thereby providing the ingredients for an analogous diametric-drive acceleration. Even if the initial spectrum locates in a single diffraction region, the other region is also accessible by means of self-phase modulation that enables a spatial spectral broadening. In real space, we expect that the probe beam spontaneously bends under the action of a nonlinearity [Fig. 1(b)]. Such a feature is characterized by the movement of the output beam pattern from the linear to the nonlinear evolution. Meanwhile, the spatial spectra for the two outputs are compared to examine the momentum change brought by the acceleration. As shown in previous work, the two components experiencing normal and anomalous diffractions tend to move along opposite directions in the momentum space during interaction [13].

Our experiments are carried out in a 1D photonic lattice (with a lattice constant of $\Lambda = 6.8 \mu\text{m}$) that is fabricated by titanium in-diffusion in a nonlinear photovoltaic copper-doped lithium niobate crystal (LiNbO_3). The associated setup is similar to that in Ref. [20]. A vertically orientated stripe beam is focused by means of a $10\times$ objective to probe this periodic optical structure. The stripe beam is picked out from a broad beam illuminating a programmable spatial light modulator (SLM) imposed with a phase pattern shown in Fig. 1(c), and is further delivered to the front focal plane of the objective through a $4-f$ system. Consequently, the beam at the input facet of the sample is a horizontally elongated Gaussian-like beam [Fig. 1(c)] covering several lattice sites. The tilting angle of the beam relative to the waveguide is readily controlled by shifting the phase pattern on the SLM horizontally.

In the first experiment, a tilting probe beam with a momentum about $q = -0.75\pi/\Lambda$ is employed, close to a zero-diffraction point of the first Bloch band in the first Brillouin zone (BZ). Figure 1(d) presents the measured output beam exiting from a linear propagation of 1.4 cm distance at a very low input power. After turning up the input power to $4 \mu\text{W}$ for generating sufficient self-defocusing nonlinearity [22] in the LiNbO_3 crystal, the nonlinear output beam exhibits a rightward shift. The corresponding outputs are summarized in a 1D configuration in Fig. 2(a) by integrating the beam patterns along

the y direction. The resulting shift is attributed to the action-reaction symmetry breaking, where both the components in the normal and anomalous regions prefer to accelerate along the same transverse direction during the nonlinear interaction. The acceleration in turn leads to a momentum change that can be revealed in the spatial spectrum of the output. Under the action of the nonlinearity, the spectrum in the linear case splits into two parts that move towards the center and left boundary of the first BZ [Fig. 2(b)]. Meanwhile, the right boundary of the first BZ is excited via the effect of Bragg reflection. Once the momentum of the input is reversed (i.e., $q = 0.75\pi/\Lambda$), the main features of the captured output are reversed accordingly (not shown here).

To obtain an insight into our observations, we perform numerical simulations by employing the 1D nonlinear Schrödinger equation that models the beam propagation in a photonic lattice [22]:

$$i \frac{\partial \psi}{\partial z} + \frac{1}{2nk_0} \frac{\partial^2 \psi}{\partial x^2} + k_0 A \cos^2(\pi x/\Lambda) \psi = \Gamma \frac{|\psi|^2}{1 + |\psi|^2} \psi, \quad (1)$$

where ψ is the complex amplitude of a light, x (or z) is the transverse (or longitudinal) coordinate, k_0 is the wavenumber in the vacuum, and n is the unperturbed refractive index of the crystal. The periodic potential associated with the photonic lattice is approximately modeled by a \cos^2 function with A being the lattice modulation depth. The nonlinear coefficient is $\Gamma = k_0 n^3 \gamma_{33} E_{pv}/2$, where γ_{33} is the electro-optical coefficient, and E_{pv} is the photovoltaic field. Figures 2(c) and 2(d) present the numerical outputs by employing the parameters similar to the experimental conditions. They have a good agreement with the observations. In a longer distance, the numerical beam propagation exhibits an obvious self-bending [Fig. 2(e)]. The mechanism behind can be understood by further analyzing the

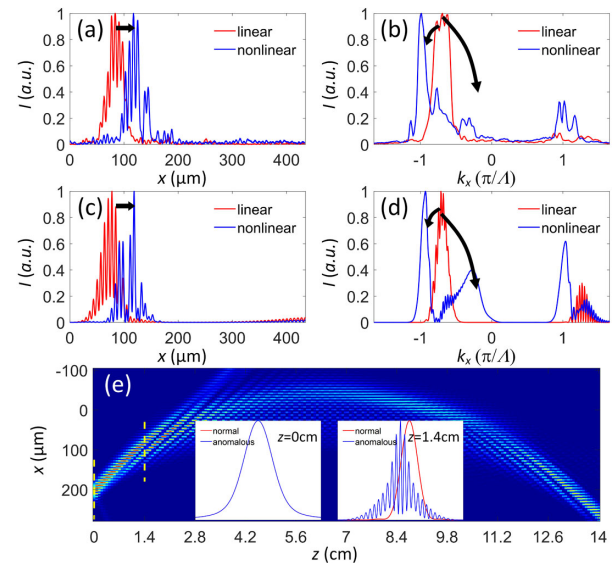


Fig. 2. (a) and (b) Experimental results of linear (red) and nonlinear (blue) outputs measured in (a) real and (b) momentum spaces for a probe beam with the initial momentum $q = -0.75\pi/\Lambda$, where the nonlinear case corresponds to the single-beam induced coherent diametric-drive acceleration; (c) and (d) numerical results corresponding to (a) and (b); (e) numerical beam propagation corresponding to (c) for a longer propagation distance (the insets show the components in the normal and anomalous diffraction regions at $z = 0$ and 1.4 cm).

real space evolution of the components experiencing different types of diffraction. Initially, the two components overlap exactly. During the nonlinear interaction, they fail to occupy the same location. Specifically, under the self-defocusing nonlinearity, the negative index change induced by the component in the anomalous (normal) diffraction region is able to repel (attract) the part experiencing the normal (anomalous) diffraction. The part in the normal diffraction region prefers to stay at only one side [here the right side as shown in the inset of Fig. 2(e)] of the other part, since its self-defocusing evolution is asymmetric near the inflection point, where the maximum beam tilting in the photonic lattice is defined. Consequently, they constitute a pair similar to that in a coherent diametric-drive acceleration [20] and move jointly in a self-accelerating manner during the following propagation.

Next, we examine the influence of the beam tilting on the spontaneous bending propagation. For this purpose, the initial momentum of the probe is set to vary from $-\pi/\Lambda$ to 0, while the input power is fixed at a constant value (i.e., $4 \mu\text{W}$). The recorded nonlinear outputs in the real and momentum spaces for different input conditions are stacked in Figs. 3(a) and 3(b), respectively. The beam center, as calculated by $\int x I dx / \int I dx$, has a considerable rightward shift for q ranging between -0.8 and $-0.6\pi/\Lambda$. In these regions, the spectrum exhibits a splitting process similar to that in Fig. 2(b). The components experiencing normal and anomalous diffractions tend to accelerate in the same direction during the nonlinear propagation, leading to a beam center shift at the output. In contrast, a single type of diffraction dominates the nonlinear evolution for q near 0 or $-\pi/\Lambda$, despite the presence of the spectral splitting; thus, the beam mainly undergoes a commonly seen self-defocusing or -focusing propagation [23]. To realize the maximum acceleration, both components in different diffraction regions should be properly divided. As inferred from the results in Fig. 3(b), there should be an optimized tilting for this task. This is verified by further analyzing the beam center shift δ from the linear to the nonlinear outputs in Fig. 3(a), i.e., $\delta = C_{\text{NL}} - C_L$, where C_{NL} and C_L are the beam centers for the nonlinear and linear outputs, respectively. The optimized

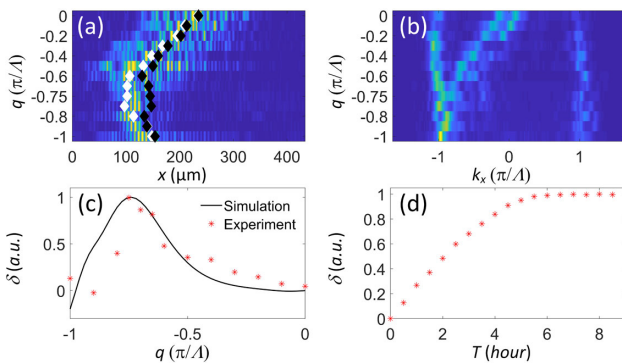


Fig. 3. (a) Experimentally measured nonlinear outputs in the real space for various initial momenta of the probe beam. The white and black diamonds mark the beam centers in the linear and nonlinear cases, respectively; (b) captured spectral distributions corresponding to (a); (c) comparison of beam center shifts from experiment [extracted from (a)] and those from numerical simulations; (d) beam center shift at the output during a temporal evolution by employing a probe with $q = -0.75\pi/\Lambda$. Such a temporal change can be translated into a change in terms of nonlinear strength (explained in the main text).

value of q appears at about $-0.75\pi/\Lambda$ [Fig. 3(c)], which also agrees with the numerical calculations. Furthermore, we employ this tilt to examine the influence of the nonlinear strength on the spontaneous diametric-drive acceleration. By fixing the power value (i.e., $4 \mu\text{W}$), the temporal evolution of the output can be translated into the scenario of increasing the nonlinear strength, since the nonlinear coefficient is time (T) dependent, i.e., $\Gamma(T) = \Gamma_0[1 - \exp(-T/\tau)]$, where Γ_0 is the nonlinear coefficient for steady states, and τ is a constant indicating the buildup time [24]. As time flies, the beam center shift continuously increases until a steady state is reached [Fig. 3(d)]. In other words, stronger nonlinearity can lead to a larger bending propagation.

Finally, incoherence is taken into account for studying the spontaneous diametric-drive acceleration. The coherent degree appearing in the nonlinear interaction is reduced by altering the phase pattern imposed on the SLM in a speed much faster than the nonlinear response of our sample [25]. In detail, 60 phase patterns similar to that in Fig. 1(c), but with an additional quadratic phase (expressed as αk_x^2 where the coefficient α is different for each pattern) along the horizontal direction, are cyclically played at a rate of 60 Hz. The value of α varies from -0.2 to 0.2 with a step of $0.4/59$. In general, the coherence degree of two beams with a time-dependent phase relationship is characterized via the visibility of their interference fringe i.e., $v = (\bar{I}_{\text{max}} - \bar{I}_{\text{min}})/(\bar{I}_{\text{max}} + \bar{I}_{\text{min}})$, where \bar{I}_{max} and \bar{I}_{min} are the maximum and minimum time-averaged intensity of the interference pattern, respectively. We employ this formula to characterize the coherent degree for the radiations from any two points on the light wave front at the input. Thus, the visibility V of the whole input beam produced from the incoherent superposition of 60 different Gaussian beams can be calculated by counting all the pairs of points in the wave front, i.e.,

$$V = \frac{1}{w^2} \int_0^w \int_0^w v(x_1, x_2) dx_1 dx_2, \quad (2)$$

where w is the width of the calculation window. In this way, V is estimated to be 0.9263 for the resulting partially coherent beam used in our experiment. During measurement, the input beam was blocked after the steady state of the nonlinear evolution was reached. The nonlinear output was revisited by unblocking the same input but with a quite lower intensity (to avoid the appearance of nonlinear effect), thanks to the dark storage property of the photorefractive crystal. Then the partially coherent output was obtained by overlapping all the 60 output beam patterns associated with each frame of the movie on the SLM. Its 1D configurations in both real and momentum spaces are shown in Figs. 4(a) and 4(b). Akin to the coherent case, the partially coherent beam experiences a transverse shift, and its spectrum undergoes a splitting process where the resulting two components move to opposite directions from the location of the linear case. Accordingly, the numerical simulation in this case is performed by rewriting Eq. (1) as [25]

$$i \frac{\partial \psi_j}{\partial z} + \frac{1}{2nk_0} \frac{\partial^2 \psi_j}{\partial x^2} + k_0 A \cos^2(\pi x/\Lambda) \psi_j = \Gamma \frac{I}{1+I} \psi_j, \quad (3)$$

where ψ_j ($j = 1, 2, \dots, 60$) is the light field associated with each frame of the phase movie, and the intensity of the partially coherent beam is expressed by $I = \sum |\psi_j|^2/60$. As shown in

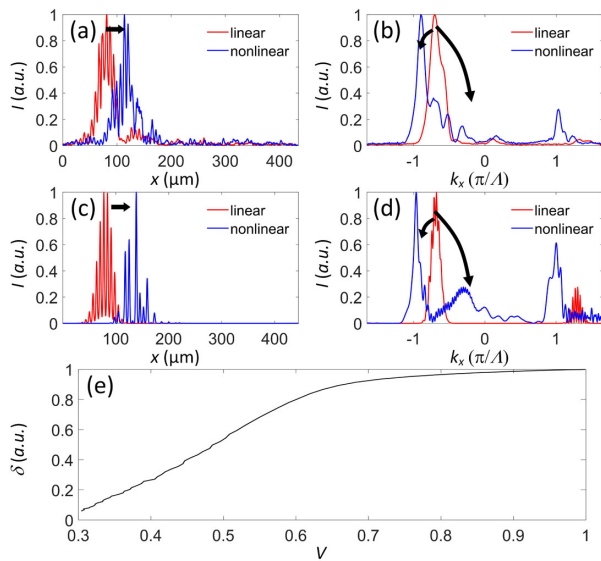


Fig. 4. Spontaneous diametric-drive acceleration triggered by a *partially coherent* probe beam with $q = -0.75\pi/\Lambda$. (a) and (b) Linear (red) and nonlinear (blue) outputs measured in the real (a) and momentum (b) spaces; (c) and (d) numerical results corresponding to (a) and (b); (e) numerically calculated shift δ of the beam center for various degrees of coherence [characterized by the visibility V defined by Eq. (2)].

Figs. 4(c) and 4(d), the numerical results are in good accordance with the measured ones. Furthermore, our simulations presented in Fig. 4(e) show that the beam center shift decreases as the coherence is reduced, indicating a weaker diametric-drive acceleration. However, for a mild incoherence degree (say, $V > 0.6$), the accelerating strength is still considerable.

In conclusion, we have demonstrated the self-bending propagation of a single Gaussian-like beam in a uniform 1D photonic lattice under a self-defocusing nonlinearity. Such a behavior originates from the spontaneous separation of the two components in the beam that experience diffractions of opposite signs under the action of the nonlinearity, then satisfying the condition for synchronized acceleration in a diametric-drive fashion. We find that there is an optimized tilting angle for the input beam to reach the maximum acceleration. In addition, our results show that a stronger nonlinearity has a positive impact on the acceleration strength. Such a spontaneous bending is further realized for a partially coherent beam, even exhibiting a considerable acceleration in a weakly incoherent regime. Compared to the scheme of two-beam excitations [13,20], the method demonstrated here is much simpler in both design and experiment for realizing a diametric-drive acceleration. This work may bring about new possibilities for beam steering and switching.

Funding. National Key Research and Development Program of China (2017YFA0303800); National Natural Science Foundation of China (61575098, 91750204); 111

Project in China (B07013); Natural Science Foundation of Ningbo (ZX2015000617).

Disclosures. The authors declare that there are no conflicts of interest related to this Letter.

REFERENCES

1. D. N. Christodoulides, F. Lederer, and Y. Silberberg, *Nature* **424**, 817 (2003).
2. R. Morandotti, U. Peschel, J. S. Aitchison, H. S. Eisenberg, and Y. Silberberg, *Phys. Rev. Lett.* **83**, 4756 (1999).
3. R. A. Vicencio, M. I. Molina, and Y. S. Kivshar, *Opt. Lett.* **28**, 1942 (2003).
4. G. Lenz, I. Talanina, and C. Martijn de Sterke, *Phys. Rev. Lett.* **83**, 963 (1999).
5. J. Wang, Z. Ye, A. Miller, Y. Hu, C. Lou, P. Zhang, Z. Chen, and J. Yang, *Phys. Rev. A* **83**, 033836 (2011).
6. T. Pertsch, P. Dannberg, W. Elflein, A. Bräuer, and F. Lederer, *Phys. Rev. Lett.* **83**, 4752 (1999).
7. T. Pertsch, T. Zentgraf, U. Peschel, A. Bräuer, and F. Lederer, *Appl. Phys. Lett.* **80**, 3247 (2002).
8. J. Meier, G. I. Stegeman, Y. Silberberg, R. Morandotti, and J. S. Aitchison, *Phys. Rev. Lett.* **93**, 093903 (2004).
9. S. Liu, Y. Hu, P. Zhang, X. Gan, F. Xiao, C. Lou, D. Song, J. Zhao, J. Xu, and Z. Chen, *Opt. Lett.* **36**, 1167 (2011).
10. R. Morandotti, U. Peschel, J. S. Aitchison, H. S. Eisenberg, and Y. Silberberg, *Phys. Rev. Lett.* **83**, 2726 (1999).
11. A. B. Aceves, C. De Angelis, T. Peschel, R. Muschall, F. Lederer, S. Trillo, and S. Wabnitz, *Phys. Rev. E* **53**, 1172 (1996).
12. L. Hadžievski, A. Maluckov, M. Stepić, and D. Kip, *Phys. Rev. Lett.* **93**, 033901 (2004).
13. Y. Pei, Y. Hu, C. Lou, D. Song, L. Tang, J. Xu, and Z. Chen, *Opt. Lett.* **43**, 118 (2018).
14. M. Wimmer, A. Regensburger, C. Bersch, M. A. Miri, S. Batz, G. Onishchukov, D. N. Christodoulides, and U. Peschel, *Nat. Phys.* **9**, 780 (2013).
15. S. Batz and U. Peschel, *Phys. Rev. Lett.* **110**, 193901 (2013).
16. G. A. Siviloglou, J. Broky, A. Dogariu, and D. N. Christodoulides, *Phys. Rev. Lett.* **99**, 213901 (2007).
17. M. Zhang, G. Huo, H. Zhong, and Z. Hui, *Opt. Express* **25**, 22104 (2017).
18. H. Sakaguchi and B. A. Malomed, *Phys. Rev. E* **99**, 022216 (2019).
19. A. Alberucci, C. P. Jisha, U. Peschel, and S. Nolte, *Phys. Rev. A* **100**, 011802 (2019).
20. Y. Pei, Y. Hu, P. Zhang, C. Zhang, C. Lou, C. E. Rüter, D. Kip, D. Christodoulides, Z. Chen, and J. Xu, *Opt. Lett.* **44**, 5949 (2019).
21. F. Di Mei, P. Caramazza, D. Pierangeli, G. Di Domenico, H. Ilan, A. J. Agranat, P. Di Porto, and E. DelRe, *Phys. Rev. Lett.* **116**, 153902 (2016).
22. F. Chen, M. Stepić, C. E. Rüter, D. Runde, D. Kip, V. Shandarov, O. Manela, and M. Segev, *Opt. Express* **13**, 4314 (2005).
23. H. S. Eisenberg, Y. Silberberg, R. Morandotti, and J. S. Aitchison, *Phys. Rev. Lett.* **85**, 1863 (2000).
24. E. Smirnov, M. Stepić, C. E. Rüter, V. Shandarov, and D. Kip, *Opt. Lett.* **32**, 512 (2007).
25. P. Zhang, S. Huang, Y. Hu, D. Hernandez, and Z. Chen, *Opt. Lett.* **35**, 3129 (2010).